INDC(CCP)-81/U

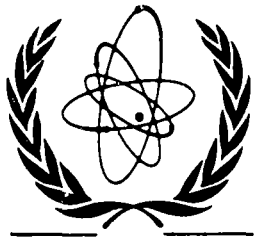

International Atomic Energy Agency

INDC INTERNATIONAL NUCLEAR DATA COMMITTEE

THE ENERGY SPECTRUM OF NEUTRONS FROM SPONTANEOUS FISSION OF ^{252}CF IN THE ENERGY RANGE 0.5-7 MEV

G.V. Kotel'nikova, B.D. Kuz'minov, G.N. Lovchikova,
O.A. Sal'nikov, N.N. Semenova, V.S. Nesterenko,
A.M. Trufanov, N.I. Fetisov

Institute of Physics and Power Engineering
(FEI)

Translated by the IAEA
May 1976

Reproduced by the IAEA in Austria
June 1976
76-3979

INDC(CCP)-81/U

FEI-575

THE ENERGY SPECTRUM OF NEUTRONS FROM SPONTANEOUS FISSION OF ^{252}CF IN THE ENERGY RANGE 0.5-7 MEV

G.V. Kotel'nikova, B.D. Kuz'minov, G.N. Lovchikova,
O.A. Sal'nikov, N.N. Semenova, V.S. Nesterenko,
A.M. Trufanov, N.I. Fetisov

Institute of Physics and Power Engineering
(FEI)

Translated by the IAEA
May 1976

ABSTRACT

The energy spectrum of neutrons from californium-252 was measured using the time-of-flight method.

The form of the spectrum accords with a Maxwellian distribution, within the limits of experimental error, for T = 1.46 ± 0.02.

INTRODUCTION

Thanks to its high specific neutron yield (of the order of 2.2×10^6 n/sec.μg), ^{252}Cf can be used even in small quantities to provide neutron sources of reasonable strength, without any serious distortion in the primary spectrum. This type of source is thus receiving considerable attention. Neutrons from californium-252 have many research applications. Reference can be made to two specific instances. One of them is the study of prompt fission neutron emission. The mechanism of prompt fission neutron emission has, in fact, not yet been thoroughly studied. Some 80-90% of fission neutrons are emitted from moving fragments isotropically in a co-ordinate system associated with the fragment. The mechanism of emission of the remaining fission neutrons (10-20%) is still not clear.

Studying the energy and angular distributions of fission neutrons constitutes one way of investigating the mechanism of their origin. The spontaneous fission of californium-252 affords great experimental possibilities for such research.

A second application is to use the spectrum of californium-252 spontaneous fission neutrons as an international standard. The use of such a standard will considerably simplify the comparison of spectrometric measurements made by different authors in studying fission neutron spectra, neutron inelastic scattering spectra, etc.

The importance of the neutron spectrum of californium-252 as a standard depends entirely on how accurately the spectrum is known. A more exact study of the characteristics of prompt neutrons from spontaneous fission of californium-252 has therefore become an urgent practical need. Many measurements have already been made [1-12] using various differential and integral techniques, but the results obtained by the experimenters are not in good agreement. The spread in the results is greater than the measurement errors which the authors associate with their work. With regard to the spectrum of prompt neutrons from californium-252, it is at present known that the measured spontaneous fission neutron spectra can be divided into two groups with average values

$$\bar{E}_n = 2.10 \text{ MeV and } \bar{E}_n = 2.37 \text{ MeV.}$$

Not all the spectra observed conform to the Maxwellian formula $N(E) = E^{\frac{1}{2}}\exp(-E/T)$ (1) where E is the energy of the emerging neutron and T is the nuclear temperature, although most experimenters point out that the spectrum can be well described by this distribution above 0.5 MeV, when the temperature T corresponds to the mean energy in accordance with the expression $\bar{E} = 3/2T$.

It should be stressed that the measured neutron spectrum is obtained by adding the spectra of neutrons emitted by nuclear fragments of widely differing mass and kinetic energy. Hence representation of the neutron energy spectrum by a Maxwellian distribution does not have any profound physical significance, but it does provide a convenient parametric description. It is thus not to be expected that the experimental data will be in complete agreement with a Maxwellian distribution over the entire range of fission neutron energies.

The fine structure observed in the studies is regarded as due to weak groups of delayed neutrons [13, 14]. The authors usually compare their measurements at different temperatures T to assess the agreement. With the californium-252 spectrum as standard, this criterion is not satisfactory for determining the agreement between spectral shapes, since T can differ in the various parts of the spectrum for the reason given above.

Various reasons for the spread in the data of different authors are known. They are related to the fact that each author uses his own neutron detector efficiency curve. Methods of measuring and of calculating the curve differ and, hence, the possible errors also.

The spread is also due to the possible detection of gamma quanta (in addition to neutrons), the different circumstances of fission fragment detection, background counting inaccuracies, inaccuracies in the calibration of the energy scale, and different ways of making corrections.

The purpose of the present work was to measure the energy distribution of prompt neutrons from californium-252 fission over a wide range of energies, and special attention was paid to the above-mentioned causes of inaccuracy. The measurements were made using the time-of-flight method, which yields the fullest and most reliable data.

Measurement methods

Figure 3 shows a block diagram of the experimental set-up. A californium-252 fission source of intensity ~ 1 x 10^4 fissions per second was prepared by electrodeposition on a thin tantalum foil. The diameter of the layer of californium-252 was 7 mm. The foil with the layer of californium was placed inside a vacuum chamber made of 1 mm thick aluminium. At a distance of 1 mm from the californium layer a semiconductor counter was positioned for purposes of fission fragment detection. The silicon surface-barrier detector employed was made of material with a specific resistance of 300 ohm.cm and a working surface diameter of 20 mm. Pulses formed by fission fragments in the detector were separated from those caused by alpha particles and were shaped in a special circuit. After passing through a delay line, these pulses served as stop signals. For neutron detection use was made of a scintillation counter consisting of a ZhS-20 liquid scintillator (in an aluminium container of diameter 60 mm and length 60 mm) incorporated in an assembly employing a pair of FEU-36 photomultipliers connected in coincidence. To reduce the background of scattered neutrons and gamma quanta the detector was placed in a collimator consisting of a layer of paraffin wax with lithium-6 hydride. A lead shield, 100 mm thick, surrounding the detector on three sides, screened it from gamma rays. In the path of the fission neutrons the thickness of lead was 10 mm. The flight length was 140 cm and the time analyser had 512 channels.

Since the amplitude and time characteristics of the semiconductor counter change under the influence of radiation [15], its operation was periodically checked during the experiment. The energy spectra of the fission fragments were periodically recorded using a "Nokia" analyser. Figure 2 shows spectra corresponding to equal periods of operation of one of the semiconductor detectors employed. At the same time as the fission neutron spectra were measured, the number of fragments per unit time was counted. When this number had decreased by 1.5% of the initial value, the counter was replaced by another, although the time resolution in the neutron spectrum was the same as before. The integral radiation dose to each counter during the period of the experiment was:

Fragments - 2.7 x 10^8 fragments/cm^2,

Neutrons - 5 x 10^8 n/cm^2.

The total operating time of one counter was ~ 24 hours, and the count per unit time was 5×10^5 frag./min. During the measurements the threshold stability of the neutron detector was checked against the pulse count from a ^{241}A source. During the latter procedure the neutron detector was screened against californium-252 neutrons by a copper cone 50 cm in length.

Electronics

Figure 3 shows a block diagram of the electronic apparatus used in measuring the neutron time spectra. In view of the high rate of fission fragment counting by the semiconductor detector, the time converter was triggered by pulses from the neutron detector (trigger pulses). The signals from the detector were passed to the input of a fast discriminator and those from the output of a fast-coincidence circuit in the same unit to the analogue-digital time converter described in Ref. [16]. The "stop" signal for fission fragments from the semiconductor detector was obtained using a shaper with time marking at the pulse front. Since the amplitude and time characteristics of semiconductor counters change under irradiation [15], this method gives better results than forming the time-marking signal at the instant the zero line is intersected. Pulses from alpha particles are eliminated using a discriminator with regulated threshold. The block circuit of the shaper is such that the shaping device simultaneously receives the input signal (after the limiting amplifier) and the standard signal from the discriminator output. The shaper threshold is set as low as possible in relation to the pulses from the limiting amplifier output, which are raised on a "pedestal" of height equal to the amplitude of the output signals from the discriminator. This minimizes the time scatter of the output "stop" pulses and ensures rapid action of the shaper without distortion due to a high background of alpha-particle pulses. Figure 4 shows the schematic diagram of the time-mark signal shaper ($T_{13} + T_{22}$) and of the linear channel for amplitude analysis of fission fragment pulses. In addition to a fast-current amplifier ($T_1 - T_5$), this channel includes a linear discriminator ($D_1 - D_2$), an expander (D_3, C = 51 pF) and an output amplifier ($T_8 + T_{12}$).

The time resolution of the shaper was determined experimentally using a layer of ^{252}Cf located between two silicon surface-barrier counters, and was found to be ≤ 2 nsec.

The shaped signals from this circuit go to the input of the time converter. Pulses from the time converter output go to the storage address detector.

Determining the detector efficiency and other characteristic of the spectrometer

Detector efficiency

The discrepancies between the californium-252 neutron spectra as measured by different authors may be due to inaccuracies in the neutron detector efficiency curves employed. In our work, therefore, special care was taken in measuring and studying the relative efficiency of the neutron detector. The detector efficiency was measured on a time-of-flight spectrometer [17], with the EGP-IOM accelerator at the Institute of Physics and Power Engineering. A block diagram of the experimental set-up is shown in Figs 5 and 5a. The source of neutrons was the $T(p,n)^3He$ reaction, whose differential cross-section is now accurately known (~ 3%), both for the neutron emergence angle and for a wide range of proton energies [18, 19].

To determine the relative efficiency the neutron spectra from the above-mentioned reaction were measured at different angles ϑ, i.e. the angular distribution of the neutron yield was measured as a function of ϑ and of the energy of the incident protons.

The neutron yield obtained for a given angle, taking into account the background, is $S = \sigma(\vartheta) \varepsilon(E_n)$ (2)

where S = area of the neutron peak;

$\sigma(\vartheta)$ = differential cross-section of the T(p,n) reaction;

$\varepsilon(E_n)$ = detector efficiency for neutrons of energy E_n.

Knowing $\sigma(\vartheta)$, we can obtain $\varepsilon(E_n)$ experimentally.

Nine sets of independent measurements were carried out at flight length L = 2 m, three of them with proton energy E_p = 3.3 MeV, one with E_p = 3.9 MeV, one with E_p = 5 MeV, one with E_p = 6 MeV and three with E_p = 7 MeV. Two sets of measurements with E_p = 3.3 MeV were performed at L = 2.75 m. In each set of measurements the neutron spectra were measured repeatedly for 11 angles of emergence between 0° and 150° at intervals of 15°.

The purpose of making such a large number of measurements was to ensure that the results obtained were reproducible, and also to cover the widest possible energy range in determining efficiency and to get satisfactorily overlapping efficiency points in going from one proton energy to another. Three different monitors were used simultaneously: (1) an all-wave counter, positioned at an angle of 90° to the axis of the proton beam; (2) a scintillation detector, similar to the main detector, positioned at an angle $\vartheta = 60°$ to the direction of proton propagation and recording by time-of-flight only the peaks (cut off by a special electronic circuit) of neutrons from the T(p,n) reaction; (3) a current integrator.

To determine the nature of background, the measurements were repeated with the same targets under the same conditions but using burnt tritium. The current integrator was used as monitor. The tritium from the targets was burnt out by evaporation in a vacuum at 400°. Before working with the burnt targets the burn-out purity was checked. The reason for this is that making measurements using only a shielding cone was not satisfactory for determining the background of scattered neutrons in the room. At proton energies E_p = 5, 6, 7 MeV an important contribution stems from the accompanying reactions Ti(p,n) and Mo(p,n) on the base material of the target. The target width differed in the measurements with different values of E_p. For E_p = 3.3 MeV, 3.9 MeV and 5 MeV, a titanium-tritium target was used (1.4 mg/cm^2). The energy spread of the protons due to the thickness of the target was 1.4 x 72 keV = 100 keV, 1.4 x 63 keV = 88 keV and 1.4 x 51 keV = 71 keV respectively. For proton energies E_p = 6 and 7 MeV, the target thickness was 2 mg/cm^2 and the corresponding energy spreads were 2 x 46 keV = 92 keV and 2 x 40 keV = 80 keV. Figures 6-8 show typical neutron spectra from the T(p,n) reaction for an angle $\vartheta = 60°$. E_p = 3.3 and 6 MeV. Each set of measurements was analysed in the following manner:

(1) The neutron peak was separated from the background neutrons and gamma quanta on the time scale;

(2) A correction was made by calculation for the dead-time of the spectrometer using the formula:

$$p = \frac{t}{t - \sum_i N_i \tau_i} \qquad (3)$$

where t = spectrum measuring time,

N_i = number of counts in channel i,

$\tau_i = 0.25 \cdot i + tp$, where tp is the access time to the memory of the information circuit. This correction varies between 6 and 16%;

(3) Account was taken of the attenuation of the neutron flux in the material of the target holder and in the target base material. The magnitude of this correction depended on the angle of emergence of the neutrons and the maximum correction was 19% for an angle of 90°. For angles of 90° and 120°, the correction was ~ 7%, and for 45° and 135° it was < 3%.

Since 2–8 spectra were obtained for each specific neutron angle of emergence in a given set of measurements, these spectra were either first summed and then processed globally (referred to a unit monitor), or else each spectrum was processed separately – as in the case of E_p = 3.3 MeV – and the results then averaged. Processing was carried out simultaneously from the readings of 3 monitors and the results were then normalized and averaged in order to reduce the error due to the functioning of the monitors. The efficiency curves for each set of measurements were first obtained using the relative values of $\sigma(\vartheta)$ from Refs [18, 20, 21]. If several works dealt with a particular value of E_p, the calculation was based on all the data and the results were averaged. When Lieskien's recommended data [19] were published for the absolute differential cross-section values, we repeated the efficiency calculations taking these data into account. In this way we obtained nine efficiency curves for different overlapping energy ranges. These curves were normalized for the common areas. Figure 9 illustrates an efficiency curve in which almost every point has been obtained by averaging several points of approximately the same energy and value. The accuracy of the individual points in the efficiency curve obtained depends mainly on the accuracy of the recommended values used for $\sigma(\vartheta)$, the differential cross-sections of Ref. [19].

In Ref. [18] at E = 6 MeV and 7 MeV, an accuracy ≃ 3% is quoted for $\sigma(\vartheta)$. At other values of E_p, Refs [20, 21] quote an accuracy of ~ ± 10% for the relative value of $\sigma(\vartheta)$. The statistical error of the readings of the main detector for a minimum set was ~ 0.3%. The statistical error of the readings of each separate monitor was not more than 0.6%. The error in separating the neutron peak from the background depends on the magnitude of the background and on its form. In the worst case, with E_p = 7 MeV for reverse angles the error may reach a maximum value of ~ 5%. The errors due to possible inaccuracies in making the corrections are small, since the corrections themselves are only small. The triangles and crosses in the same figure indicate the efficiencies obtained when describing the experimental data by the analytical methods given in Refs [24, 25].

With the method of Ref. [24] the curve is a rational function

$$\varepsilon(E) = P_N(E) / Q_M(E) \qquad (4)$$

the parameters of which are obtained by the method described in Ref. [24], using a second order Pade approximation. In expression (4), P_N and Q_M are polynomials of orders M and N, and the coefficients are descriptive parameters. In the case considered, the optimal approximation of the experimental data was obtained with M = N = 2. After separating the constant part, expression (4) can be written in the form:

$$\varepsilon(E) = C + \frac{A + B(E - E_0)}{(E - E_0)^2 + \frac{\Gamma^2}{4}} \qquad (5)$$

where the parameters have the following values:

C = 2.7383, A = 2.579627

B = 2.7144, E_0 = 0.8835

$\Gamma/2$ = 1.1365

In the method of Ref. [25] the curve is the result of calculating the efficiency by the formula:

$$\varepsilon(E) = \sum_{K=0}^{n_o} a_K P_K(E) \qquad (6)$$

where $P_K(E)$ = orthogonal Chebyshev polynomials;

a_K = coefficients obtained by applying the least squares method to the available experimental data;

n_o = optimal degree of the polynomial as chosen using the Fisher criterion.

In calculating the parameters of the curve, each experimental point is given a weight inversely proportional to the square of its absolute error

$$\omega_i = \frac{1}{\sigma_i^2}$$

As can be seen from the diagram, the analytical descriptions of the experimental dependence of detector efficiency on the energy of the incident neutrons are in good agreement with each other. The second important aspect affecting the accuracy of the neutron spectra obtained with the time-of-flight method is the accuracy of the method used to calibrate the time scale and hence also the energy scale.

The spectrometer time scale was calibrated (i.e. the channel width of the time analyser was determined) both with the aid of calibrated delay lines and, from the number of channels between the neutron and gamma-quanta peaks in the measured spectra for the $T(p,n)^3He$ reaction. To determine the mean channel width of the analyser, 220 spectra were used. A width of 1.007 nsec was obtained. The accuracy of this method of calibration was subsequently checked by measuring the neutron spectra from the Mg(p,n), Al(p,n), and Cr(p,n) reactions where each neutron peak corresponded to excitation of a particular level of the nucleus. The experimentally determined level energies did not differ by more than 30-40 keV from the calculated values (Fig. 10).

To determine the linearity of the analyser time scale, statistically distributed (in time) pulses from a detector irradiated with ^{60}Co gamma quanta were fed to one input of the converter, and to the other input periodic pulses were applied from a G5-19 generator. The measurement results are shown in Fig. 11. The differential non-linearity was 1%, and the integral non-linearity 1.1%.

The time resolution of the spectrometer, determined from the half-height width of the gamma peak, was 4–5 nsec for all the spectra measured.

The zero mark on the time scale was determined from the position of the prompt gamma-ray peak taking into account the time-of-flight of the gamma rays to the detector.

Corrections

The final results were obtained after the following corrections.

The following background components were considered:

(a) Neutron scattering by surrounding objects and air;

(b) Random coincidences between pulses from the photomultiplier (cosmic background and photomultiplier noise) and fission fragment pulses;

(c) Random coincidences between neutrons and fragments produced in other fission events;

(d) Delayed gamma quanta.

The first of these background components was excluded by using a good detector shield and by keeping the neutron source (layer of californium) away from surrounding objects. In Ref. [10] it is shown that scattering in air is small even for a path length L = 3.7 m. The second component was studied by moving the neutron detector away from the ^{252}Cf fission source. This background is uniform and during two hours of operation it amounted to 2–3 counts per analyser channel. The third component was calculated from the formula

$$\Delta N_i = \Delta t \cdot N_f \cdot \sum_{m=i+1}^{m_{max}} N_m \qquad (7)$$

where ΔN_i = number of random coincidences in channel i;

N_m = number of counts in channel m;

N_f = number of ^{252}Cf fissions per unit time;

Δt = channel width.

The highest value of this background occurred in the low-energy part of the spectrum: for $E_n \sim 300$ keV it was ~ 4%, while for $E_n \simeq 1$ MeV it was ~ 0.1%.

The delayed gamma rays are emitted by the products of californium spontaneous fission. Since the decay times of these products differ considerably, the time distribution of the gamma rays has a complex shape, and has not been adequately studied. Steps were therefore taken to reduce the effect of gamma rays on the neutron spectra. To do this the detector on the neutron source side was screened by a layer of lead of thickness 10 mm. The gamma quanta emitted by fission products with a half-life less than the time interval that can be measured by the spectrometer must create a non-uniform background. The influence of this background could be important only for the high-energy part of the spectrum. As shown in Fig. 12, however, after subtracting the uniform background between the prompt gamma-ray peaks and the neutron spectrum there remains a time interval (~ 10 nsec), in the channels of which there is practically no count - at most 1-2 counts per channel. It follows from this that the magnitude of the background due to delayed gamma rays has no influence on the shape of the spectrum.

The above analysis of background sources shows that the main part of the background has a uniform distribution and that it is non-uniform only for the part of the spectrum below 1 MeV, owing to random coincidences between neutrons and fragments produced in various fission events. Delayed neutrons are present in the neutron spectrum but their contribution is relatively small [13, 14], so that no correction was made for them.

Under the experimental conditions in question, the semiconductor detector was situated at a distance of 1 mm from the layer of ^{252}Cf, so that approximately 10% of the fragments (emerging perpendicular to the direction of motion of the detected neutrons) were not recorded. Knowing the angular distribution of the neutrons relative to the direction of motion of the fragments [2], we find that approximately 2% of the neutrons incident on the detector were not accompanied by a stop signal from the fragment.

The effect of this fraction of neutrons on the spectrum shape was found in the following manner: we calculated the spectrum of neutrons recorded by the detector under conditions of 100% efficient fission-fragment detection, and the neutron spectrum under conditions whereby fragments were recorded taking account of the geometrical configuration of target, californium and fragment detector. The measured spectrum was corrected by reference to the ratio of the two calculated spectra.

Correction for spectrometer time resolution

As shown above, the spectra are measured with a time resolution of ~ 4 nsec. In order to allow for the effect of the resolution on the spectrum shape, a correction was made. Two methods were used for this. The correction introduced by the first method was based on the general statistical approach described by A.A. Van'kov [22, 23]. The idea of this method is to apply a priori limitations expressed in probability form (Bayes' theorum). The corresponding ALGOL programme for the M-220 machine was written by M.Z. Tarasko. A correction was made to the time spectrum. A second programme was written by E.M. Saprykin. In his method the energy spectrum is given by formula (1) for a certain value of T. The spectrum is then modified by the introduction of the resolution function and is compared with the experimental one. This procedure is repeated for changing values of T until the difference between the spectrum obtained and the experimental spectrum is minimal.

Energy resolution

The energy resolution of the measured neutron spectra is determined by the time resolution Δt (equal to the half-height width of the gamma peak) and by the uncertainty regarding the flight length due to the finite size of the detector. With Δt = 4 nsec for a detector of diameter 6 cm, the uncertainty in the flight length is

$$\Delta L = \frac{\pi D}{4\cdot 2} = \frac{\pi \cdot 6}{8} = 2{,}36 \text{ см} \qquad (3)$$

where $\frac{\pi D}{4}$ is the effective size of the detector.
The energy resolution taking account of the above-mentioned factors can be expressed by the formula

$$\Delta E = E\sqrt{\left(\frac{2\Delta t}{t}\right)^2 + \left(\frac{2\Delta L}{L}\right)^2} = E\sqrt{\frac{2\Delta t}{123L}^2 E + \left(\frac{2\Delta L}{L}\right)^2} \qquad (4)$$

Figure 16 gives the calculated values of the resolution ΔE for Δt = 4 nsec and L = 140 cm.

Errors in the energy spectrum

The neutron time spectrum is converted to an energy spectrum using the formula

$$N(E) = C\,N(t)\cdot t^3 / L^2\varepsilon \qquad (5)$$

where C = constant;

t = neutron time-of-flight for energy E and length L;

L = 140 cm (flight length);

ε = detector efficiency.

The errors calculated for the time spectra are then increased by errors due to the uncertainty in the time-of-flight Δt, in the flight length ΔL, and also by errors in the relative efficiency of the detector $\Delta\varepsilon$. The error $\Delta N(E)$ for neutron energy E given by this formula is

$$\Delta N(E) = N(E)\sqrt{\left(\frac{\Delta N(t)}{N(t)}\right)^2 + \left(\frac{3\,\Delta t}{t}\right)^2 + \left(\frac{\Delta L}{L}\right)^2 + \left(\frac{\Delta\varepsilon}{\varepsilon}\right)^2} \qquad (6)$$

where $\Delta N(t)$ = mean-square error in the time spectrum;

Δt = 0.5 nsec (channel half-width).

For the above-mentioned values of ΔL and $\Delta\varepsilon$, Fig. 15 shows the calculated errors $\Delta N(E)$ for a series of points.

Results

Neutron spectra for californium-252 fission were measured repeatedly. Altogether 26 spectra were measured. The measuring time for each spectrum was two hours. Figure 13 shows a single time spectrum.

First of all, each spectrum was processed separately without the introduction of corrections requiring complex calculations. After transfer of the time scale to the energy scale, the parameters were attached to the spectra using formula (1) and the best value of T was obtained in order to check the spread in the values. The distribution of the T values satisfied statistical requirements for all the spectra obtained.

For further calculations, a global time spectrum was obtained from 26 measured spectra, as shown in Fig. 12. The errors in the numbers of

counts in the channels of the global time spectrum were found as mean square values from the spread in the experimental values of all 26 sets. The relative mean square errors for the points in the global spectrum lie within the range 1.5–3%.

Figure 14 shows the global time spectrum corrected for the resolution using the method described in Ref. [23]. As can be seen, the irregularities in the time spectrum were all much clearer. In Refs [13, 14] attention is drawn to the presence of monoenergetic groups in the measured neutron spectra. In our time spectrum irregularities are observed, for example, at E = 2.35 and 2.76 MeV. However, these irregularities lie within the limits of measurement error, so that one cannot speak of fine structure of the spectrum, let alone try to give it a physical interpretation.

A correction was also made to the time spectrum for the integral non-linearity of the converter. A correction was made to the energy spectrum for the finite distance between the fragment detector and the layer of californium. The effects of the different corrections on the value of T was studied. In certain cases the effects are in opposition, but do not cancel each other.

Figure 15 shows the energy spectrum taking account of all the corrections dealt with in this work. The spectral points up to 1 MeV are averaged within the limits of the time resolution. The relative error of the points in the energy spectrum in the range 0.5–6 MeV is ~ 6%.

The value of T obtained from the energy spectrum by the least squares method for a Maxwellian distribution (1) is equal to 1.46 $\pm$ 0.02 in the energy range 0.5–7 MeV. Although the detector threshold is 0.2 MeV, the lower limit for determining T was set higher than 0.5 MeV, since the region below this energy is very sensitive to the accuracy with which the background is determined and this may have an effect in determining T. To find the error in the parameter T for the global spectrum, the spectra were divided into two series, each containing spectra with a similar time resolution. For each series global spectra were obtained and processed before T was derived taking all the corrections into account. From the values of T obtained the mean square error was ascertained. The error in T for the global spectrum was ~ 1.5%. The error in T as calculated from the formula in Ref. [25] is of the order of 1%

$$\Delta T = \frac{T^2\left(\sum \frac{1}{\sigma_i^2}\right)^{1/2}}{\left[\left(\sum \frac{1}{\sigma_i^2}\right)\left(\sum \frac{E_i^2}{\sigma_i^2}\right) - \left(\sum \frac{E_i}{\sigma_i}\right)^2\right]^{1/2}} \qquad (7)$$

where σ_i^2 = dispersion;

E_i = energy of point i.

In Fig. 15 the smooth curve represents the result of calculating the spectrum from formula (1) with the value of T obtained. It can be seen that agreement is fairly good over the entire energy range.

The energy spectrum on the semilog scale is shown in Fig. 17.*/

Table 1 gives values of T obtained by different authors up to 1973. It is interesting to note that the scatter in the values of this parameter exceeds the attributed errors. In our view, the main reason for this is the level of accuracy with which the neutron detector efficiency curves are determined, i.e. their shape. Unfortunately, most of the authors do not give data regarding this accuracy.

In most of the works the question of monitoring in studying efficiency curves is not touched upon, although it has an important bearing on the accuracy with which the efficiency curves are obtained.

Table 2 gives numerical values for the ^{252}Cf spectrum.

In conclusion, the authors wish to thank P.P. D'yachenko for preparing the layer of californium, the members of the A.I. Sergachev group for preparing the semiconductor detectors, A.A. Van'kov, M.Z. Tarasko and E.M. Saprykin for their help in calculating the resolution corrections, N.S. Rabotnov, V.I. Vinogradov and V.I. Platonov for their analytical description of the experimental efficiency curve, and V.M. Piksyajkin and V.G. Vorob'eva for their assistance in calculating the correction for the finite distance between the semiconductor detector and the californium layer.

*/ sic.

REFERENCES

1. Smith A.B., Fields P.R., Roberts J.H. Phys. Rev., 1957, v.108, 411.

2. Bowman H.R., Thompson S.B., Milton J.C.D., Swiatecki W.J. Phys. Rev., 1962, v.126, 2120.

3. Penner T.W. Nucl. Phys., 1961, v.23, 116.

4. Conde H., During G. Arkiv für Fisik, 1965, v.29, 313.

5. Meadows J.W. Phys. Rev., 1967, v.157, 1076.

6. ZAMYATNIN, Yu.S., KROSHKIN, N.I., MEL'NIKOV, A.K., NEFEDOV, V.N., Proc. Int. Conf. on Nuclear Data for Reactors (Helsinki), Vienna, IAEA 2 (1970) 183.

7. Werle H., Bluhm H. Proceedings of a Consultants Meeting on Prompt Fission Neutron Spectra. Vienna 1971, 65-80.

8. Green L. Americ.Nucl.Society, 1971, v.14, No.1, 119.

9. EKI, L., KLUGE, D., LATMAN, A., D'YACHENKO, P., KUZ'MINOV, B., Atomnaya energiya 33 3 (1972) 784.

10. Green L., Mitchel J.A., Steen N.M. Nucl. Science and Engineering, 1973, v.50, 257-272.

11. Knitter H.H., Paulson A., Liskien H., Islam M.M. Atomkernenergie, Bd.22, Lfg.2, 84-86, 1973.

12. NEFEDOV, V.N., STAROSTOV, B.I., SEMENOV, A.F., Proc. Second All-Union Conference on Neutron Radiation Meteorology*/, 2 Moscow (1974).

13. AVERCHENKO, V.Ya., NEFEDOV, Yu.Ya., KHILKOV, Yu.V., Proc. Second All-Union Conference on Neutron Physics, Kiev (1973).

14. NEFEDOV, V.N., MEL'NIKOV, A.K., STAROSTOV, B.I., Proc. All-Union Meeting on Neutron Physics, Kiev (1971).

15. AKIMOV, Yu.K., KALININ, A.I., KUSHNIRUK, V.F. et al., Semiconductor nuclear-particle detectors and their uses (in Russian), Atomizdat (1967).

16. KULABUKHOV, Yu.S., NESTERENKO, V.S., TIMOKHIN, A.A., Proc. Meeting of Experts from COMECON Countries, Pt. 2, (1969) 170.

*/ sic.

17. GEL'FER, G., ZELIGER, D., GLOTOV, A. et al., The pulsed regime of operation of the EGP-IOM accelerator at the Institute of Physics and Power Engineering (FEI) (in Russian), FEI Preprint No. 471 (1974).

18. McDaniels D.K., Drosg M., Hopkins J.C., Seagrave J.D. Phys. Rev. C 6 No.5, 1972, 1593-1599.

19. Lisbon K., Paulsen A. Nuclear Data Tables, 1973, vol.2, No.7, 1973, 569-613.

20. Fowler J.L., Brolley J.E. Rev. Mod. Phys.1956,v.28,No.2.

21. Wilson N.E., Walter P.L., Fossan D.B. Nucl. Phys., 1961, vol.27, 421-430.

22. VAN'KOV, A.A., Determination of radiation energy spectra from spectroscopic measurements (in Russian), Part 1, FEI Preprint No. 485 (1974).

23. VAN'KOV, A.A., Determination of radiation energy spectra from spectrometric measurements (in Russian), Part 2, FEI Preprint No. 486 (1974).

24. VINOGRADOV, V.N., GAJ, E.V. et al., FEI Preprint No. 484 (1974).

25. HUDSON, D., Statistics for physicists, Moscow (1967).

Table 1

Values of T obtained in the present work and in that of other authors

T (MeV)	Energy range of spectrum (MeV)	Reference
1,423	0,1 ÷ 9,5	7
1,44	1,5 ÷ 7	
1,40	0,1 ÷ 7	
1,43±0,02	0,7 ÷ 10	8
1,565	0,003 ÷ 15	5
1,48±0,03	0,04 ÷ 6	6
1,57	0,002 ÷ 1	9
1,39	0,3 ÷ 7	4
1,367±0,03	0 ÷ 4	3
1,56	0,5 ÷ 6	2
1,57		1
1,406±0,015	0,44 ÷ 12,68	10
1,43	0,15 ÷ 15	11
1,43±0,03	0,7 ÷ 10	12
1,46±0,02	0,5 ÷ 7	present work

Table 2

E	N	E	N	E	N
0,25	215,9±28,1	1,18	239,9±13,9	2,85	119,6±7,2
0,26	193,6±2,36	1,21	239,2±13,8	2,95	113,9±6,8
0,27	205,9±21,6	1,23	240,4±13,9	3,06	110,4±6,6
0,28	254,6±22,0	1,26	236,5±13,6	3,17	107,4±6,5
0,29	222,2±18,9	1,29	224,3±13,0	3,28	101,7±6,2
0,30	232,0±19,2	1,32	222,5±12,8	3,40	91,4±5,3
0,32	260,7±19,1	1,35	220,5±12,7	3,53	83,1±5,1
0,33	237,1±16,9	1,38	216,6±12,5	3,67	76,8±4,7
0,35	231,2±19,1	1,41	210,9±12,2	3,81	71,3±4,4
0,37	259,4±16,9	1,45	214,8±12,4	3,97	65,6±4,1
0,38	274,9±17,2	1,48	214,2±12,4	4,13	61,2±3,8
0,40	286,7±17,4	1,52	209,8±12,1	4,30	55,8±3,5
0,43	273,2±16,3	1,56	202,4±11,7	4,49	51,3±3,3
0,45	258,1±15,2	1,60	196,7±11,4	4,68	44,2±2,8
0,47	265,7±15,6	1,64	198,4±11,5	4,89	38,4±2,5
0,50	277,4±15,9	1,68	200,6±11,6	5,11	34,6±2,2
0,53	264,2±15,0	1,73	197,5±11,4	5,35	31,1±2,0
0,56	274,6±15,5	1,77	191,3±11,1	5,61	26,8±1,8
0,60	272,0±15,3	1,82	188,8±11,0	5,89	21,0±1,4
0,64	284,7±15,9	1,87	187,2±10,9	6,18	16,8±1,2
0,68	286,0±15,9	1,92	180,2±10,5	6,50	14,7±1,0
0,72	280,1±15,6	1,98	175,5±10,2	6,84	12,9±0,9
0,78	293,3±16,2	2,03	166,4± 9,7	7,22	10,4±0,7
0,83	272,3±15,1	2,09	161,9± 9,5	7,62	8,3±0,6
0,90	263,9±14,9	2,15	165,0± 9,7	8,06	6,2±0,5
0,97	255,9±14,2	2,22	160,2± 9,4	8,54	4,6±0,4
1,02	255,2±14,8	2,28	159,7± 9,4	9,06	3,5±0,3
1,04	257,0±14,9	2,35	155,4± 9,1	9,64	2,6±0,2
1,06	256,7±14,9	2,43	146,5± 8,6	10,26	1,8±0,2
1,08	250,9±14,5	2,51	136,8± 8,1	10,96	1,2±0,1
1,11	235,9±13,7	2,59	136,0± 8,1	11,72	0,7±0,1
1,13	234,5±13,6	2,67	134,7± 8,0	12,57	0,5±0,1
1,15	237,5±13,7	2,76	131,7± 7,6		

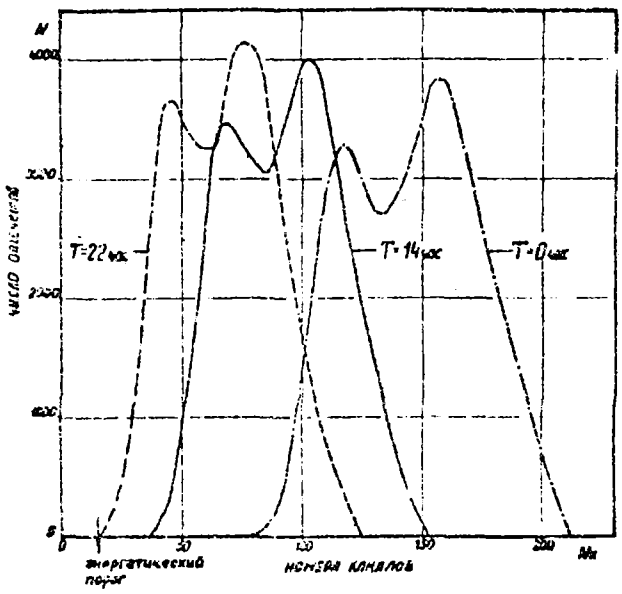
N
4000
2000
0
T=22 мс
T=14 мс
T=0 мс
0
50
100
150
200
Мк
энергетический порог
номера каналов

Fig. 2

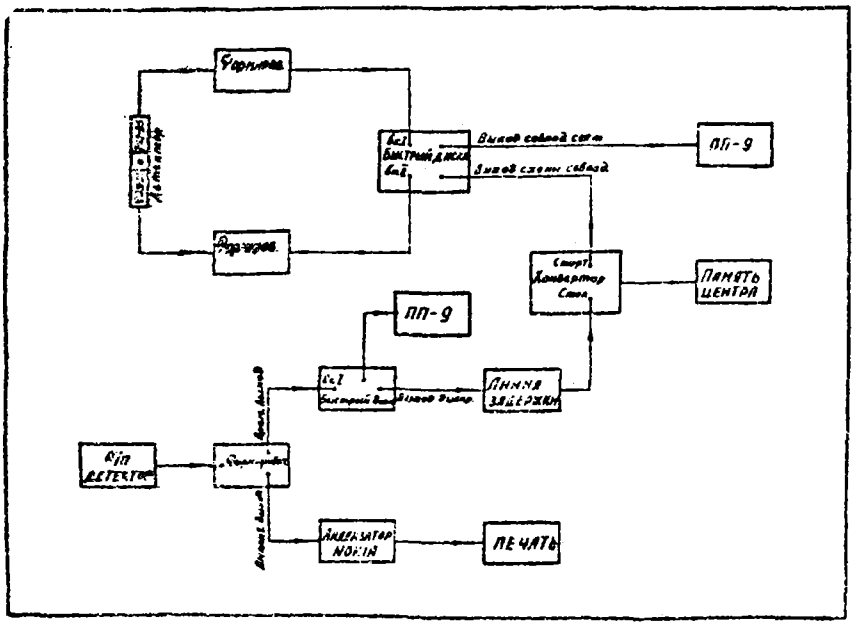
ПП-9
ПАМЯТЬ ЦЕНТРА
ПП-9
ЛИНИЯ ЗАДЕРЖКИ
ПЕЧАТЬ

Fig. 3

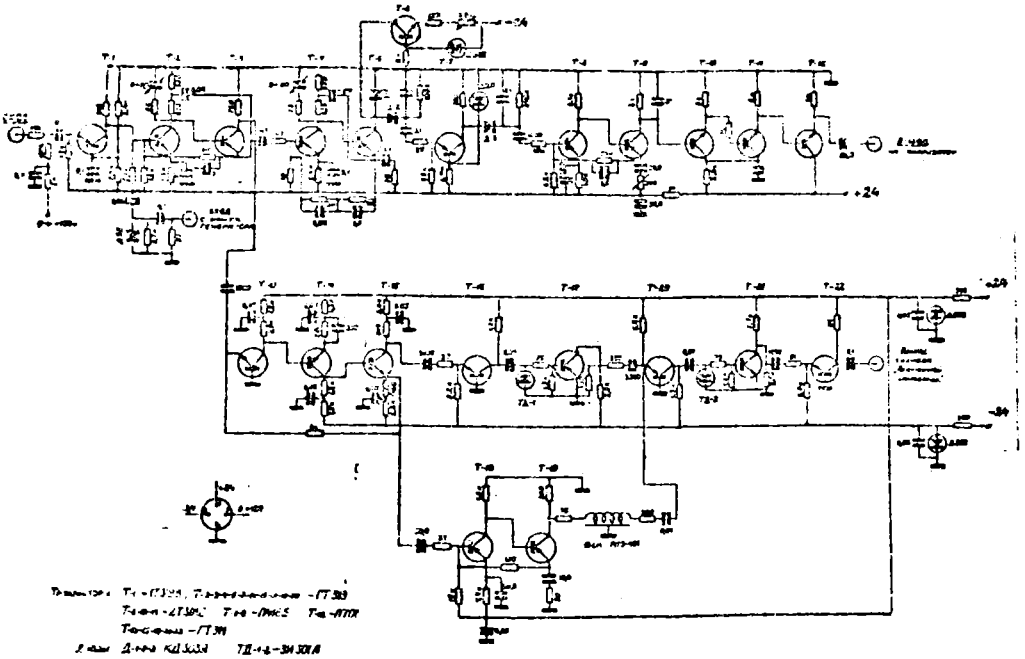

Fig. 4

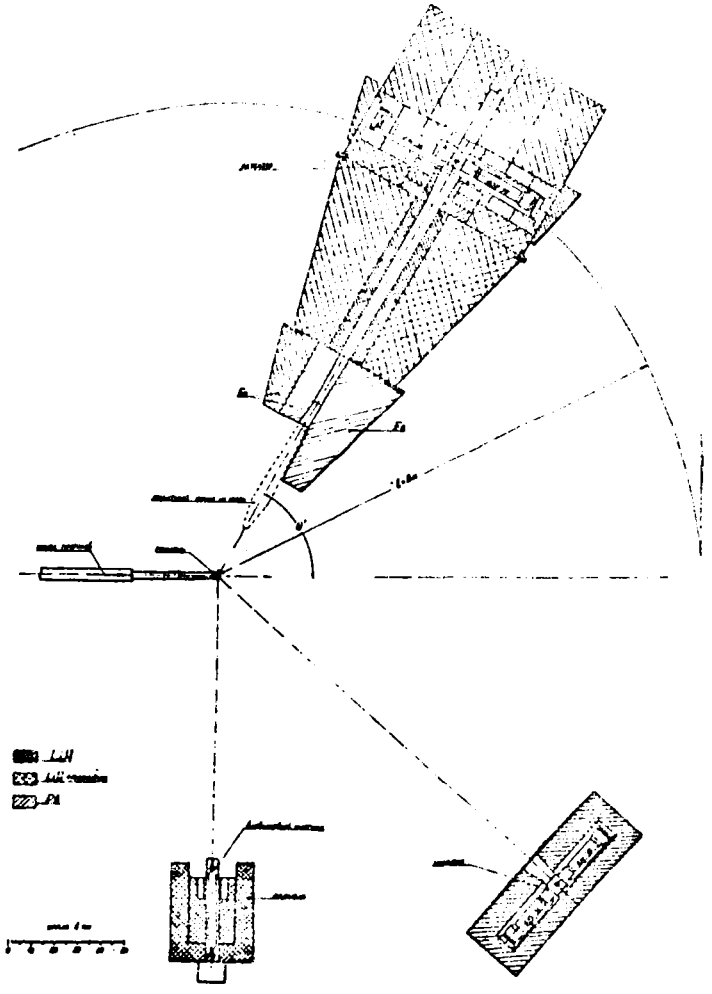

Fig. 5

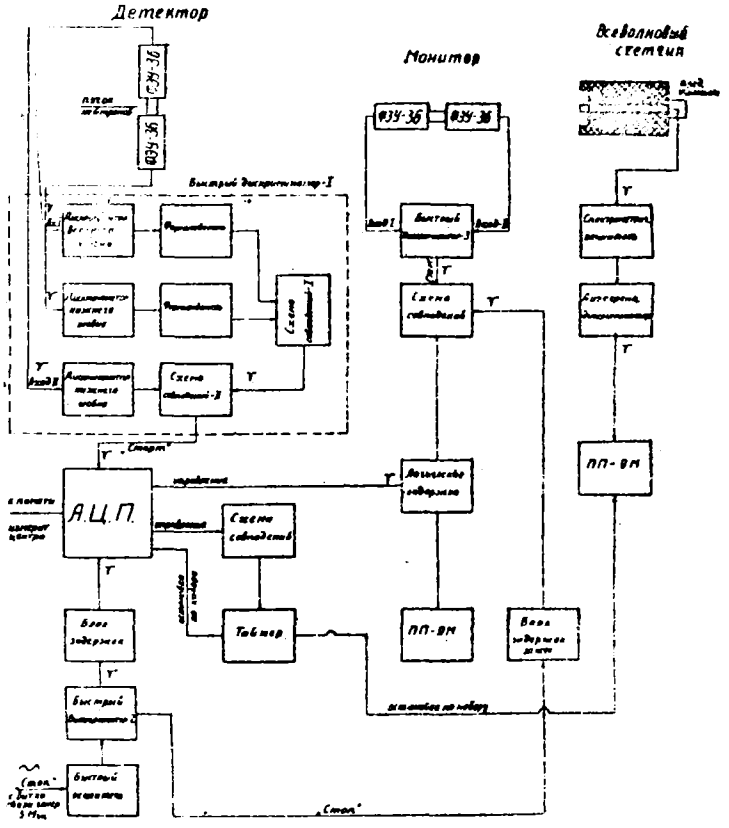
Детектор
Монитор
Всеволновый счетчик
А.Ц.П.
ПП-ВМ
Табтор

Fig. 5a

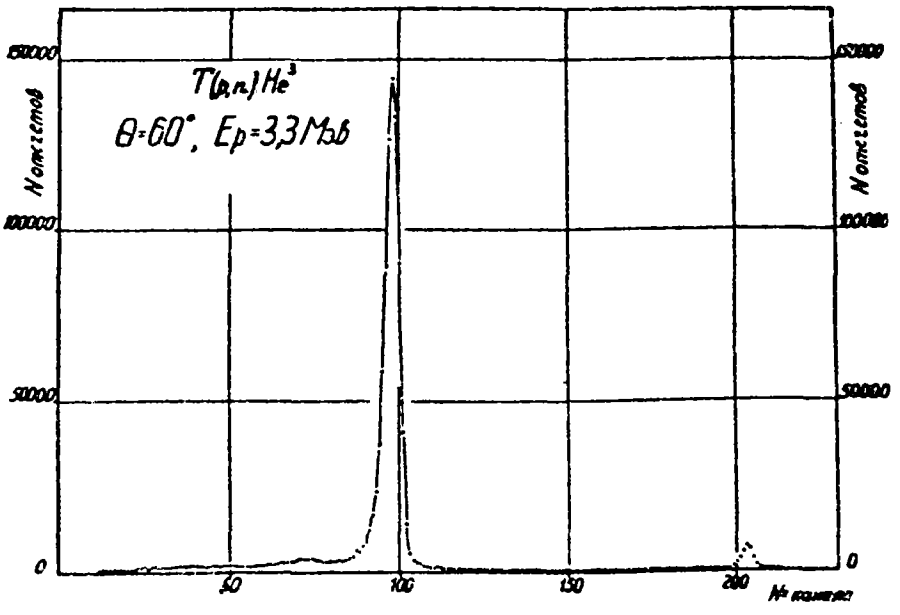
T(p,n)He³
θ=60°, Ep=3,3 Мэв
Импульсов
100000
50000
0
50
100
150
200

Fig. 6

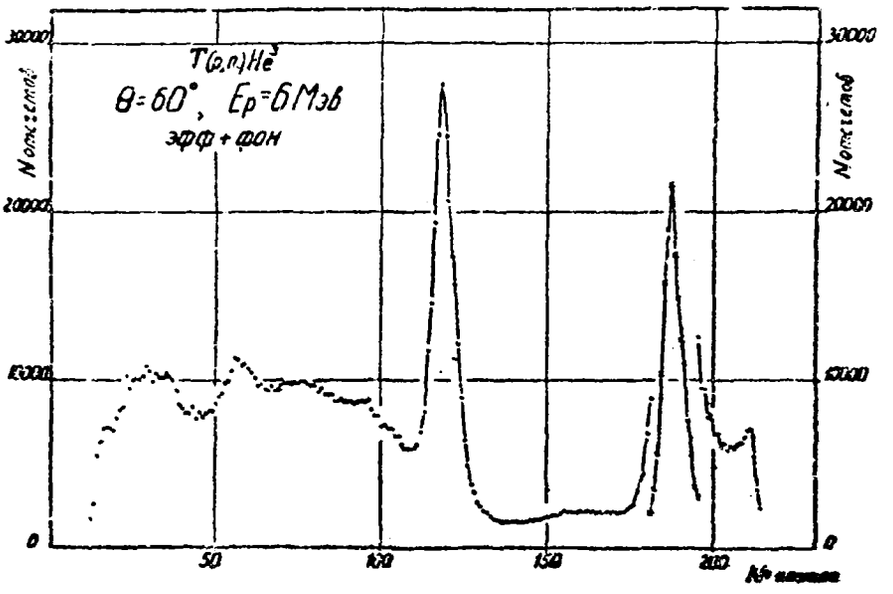
T(p,n)He³
θ=60°, Ep=6 Мэв
эфф + фон
30000
20000
10000
0
50
100
150
200

Fig. 7

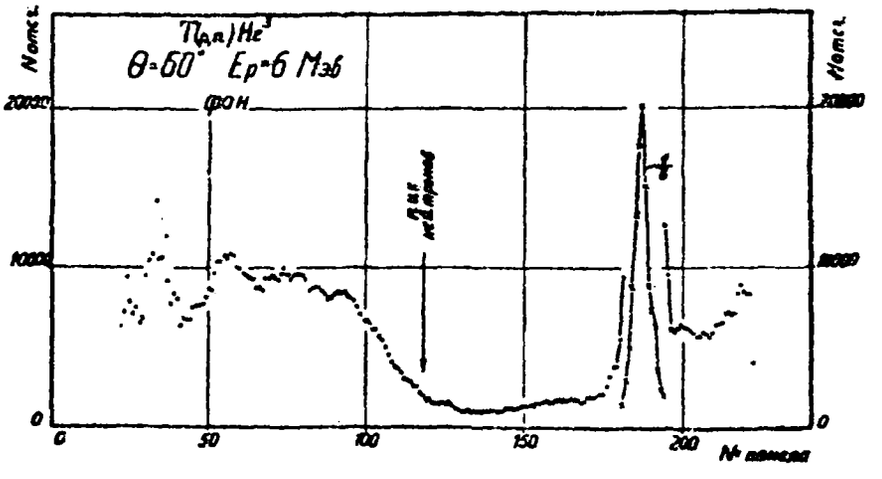
T(p,n)He³
θ=60° Ep=6 Мэв
фон
20000
10000
0
50
100
150
200

Fig. 8

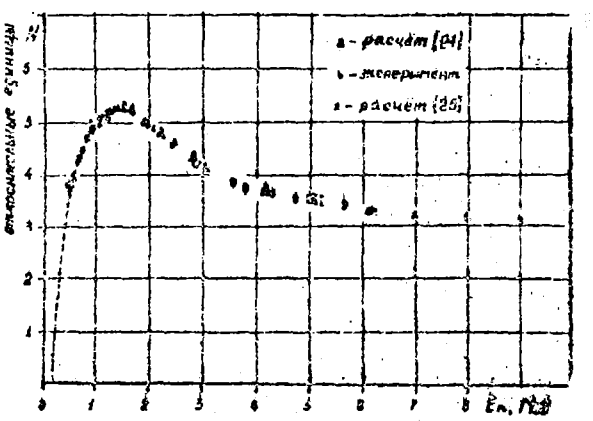

Fig. 9

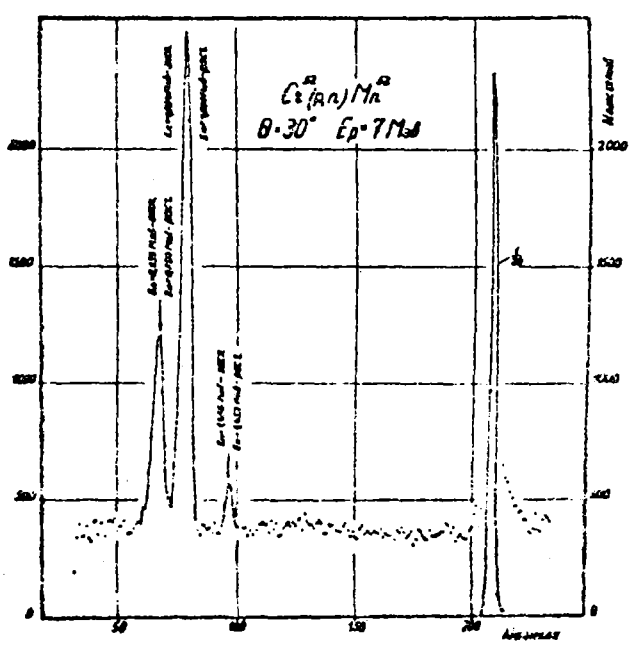

Fig. 10

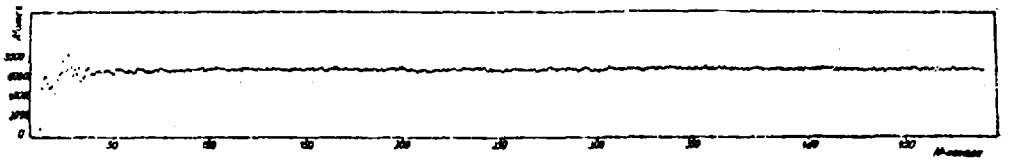

Fig. 11

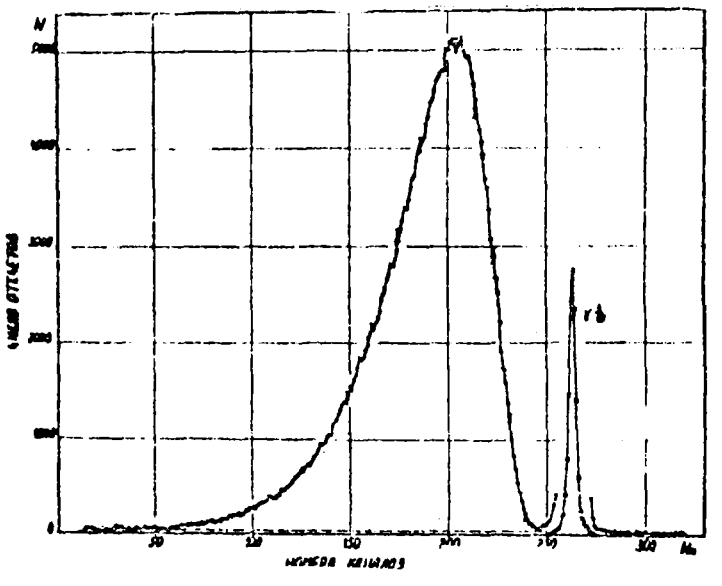

Fig. 12

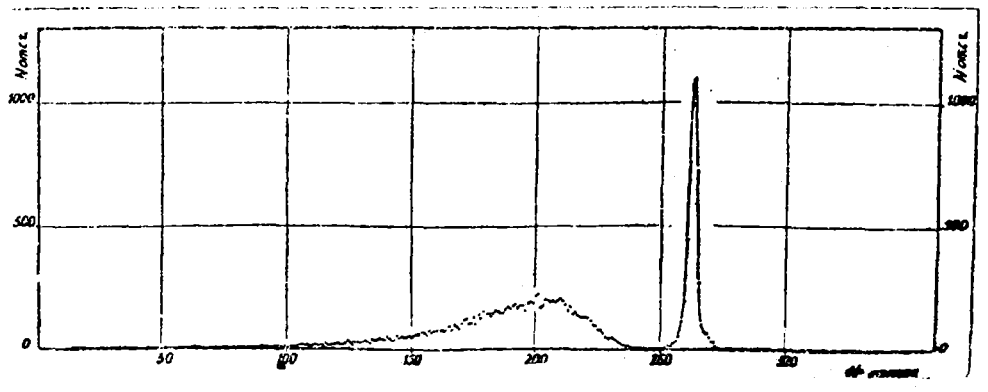

Fig. 13

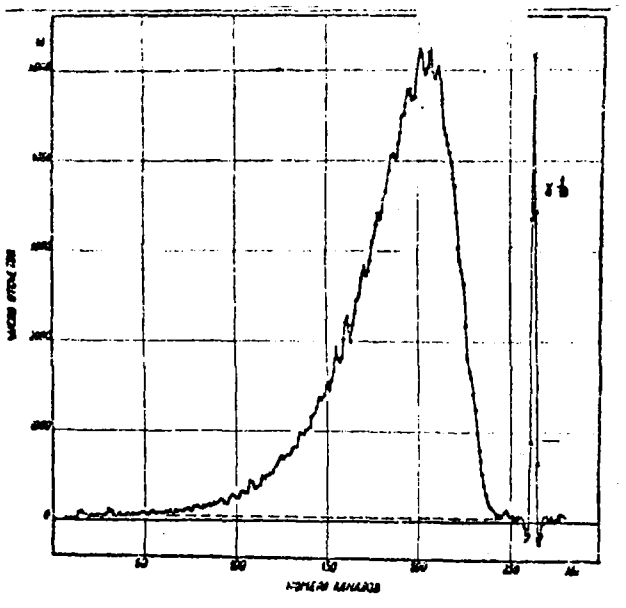

Fig. 14

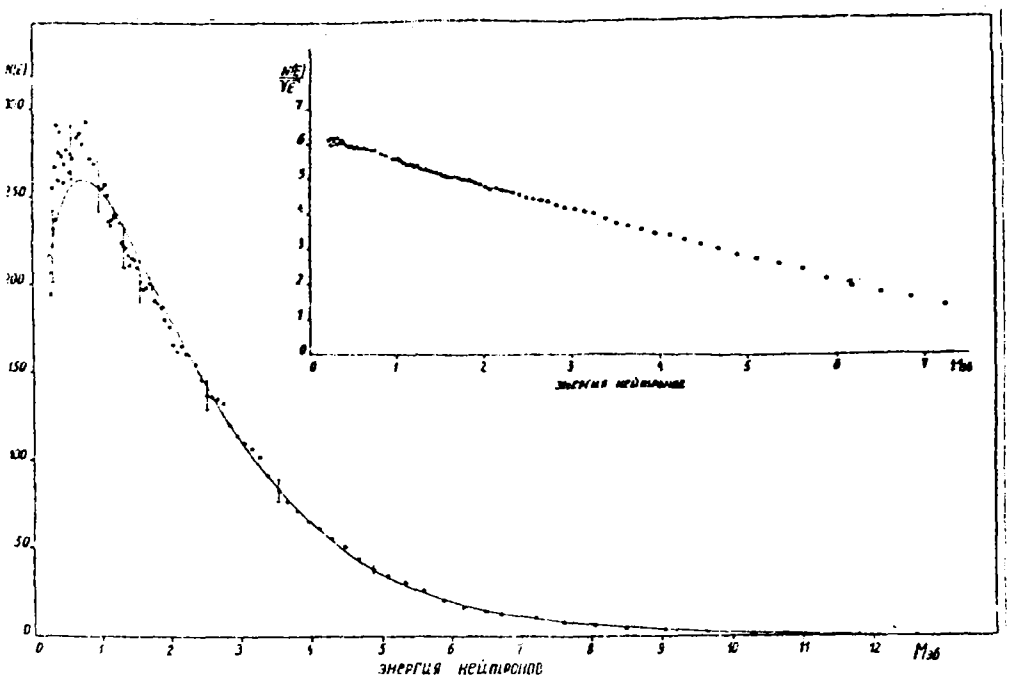
Энергия нейтронов
МэВ

Fig. 15

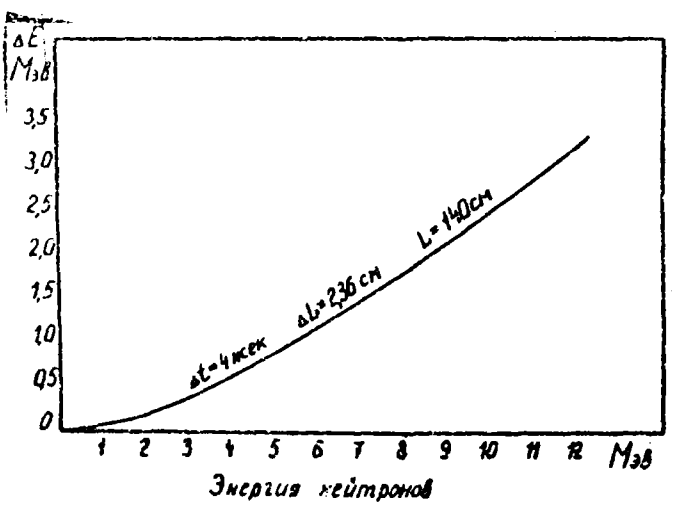
ΔE
МэВ
3,5
3,0
2,5
2,0
1,5
1,0
0,5
0
Δt=4мкек
Δl=236см
L=140см
1 2 3 4 5 6 7 8 9 10 11 12 МэВ
Энергия нейтронов

Fig. 16